

**Electronic structure and bonding at the  
Al-terminated Al(111)/ $\alpha$ -Al<sub>2</sub>O<sub>3</sub>(0001) interface: A first principles study**

**Donald J. Siegel**

Department of Physics, University of Illinois at Urbana-Champaign,  
1110 West Green St., Urbana, IL, 61801.

**Louis G. Hector, Jr.**

GM Research and Development Center,  
30500 Mound Road, P.O. Box 9055, Warren, MI 48090

**James B. Adams**

Chemical and Materials Engineering Department,  
Arizona State University, Tempe, AZ 85287-6006.

**ABSTRACT**

We have performed *ab initio* calculations to determine the bonding character of the Al-terminated Al(111)/ $\alpha$ -Al<sub>2</sub>O<sub>3</sub>(0001) interface. By using an optimized model in which all atomic coordinates were relaxed to their minimum energy positions, we have determined that Al-O bonds constitute the primary interfacial bonding interaction. Our electron localization, Mayer bond order, and Mulliken population analyses reveal that these bonds are very similar to the cation-anion bonds found in the bulk oxide, and are therefore mainly ionic, with a smaller amount of covalent character. However, there is also evidence of metal-cation bonding across the interface, a result which could be significant to understanding bonding at interfaces with other corundum-like oxides.

**INTRODUCTION**

Interfaces between metals and ceramics play a vital role in an increasingly large number of industrial applications[1]: heterogeneous catalysis, microelectronics, thermal barriers, corrosion protection and metals processing are but a few representative examples. However, experimental complications associated with the study of a buried interface, and theoretical difficulties arising from complex interfacial bonding interactions have hindered the development of general, analytic models capable of accurately predicting fundamental interfacial quantities.

One such quantity, which is key to predicting the mechanical properties of an interface, is the ideal work of adhesion,  $\mathcal{W}_{ad}$ , [1] which is defined as the bond energy needed (per unit area) to reversibly separate an interface into two free surfaces, neglecting plastic and diffusional degrees of freedom. Formally,  $\mathcal{W}_{ad}$  can be defined in terms of either the surface and interfacial energies (relative to the respective bulk materials) or by the difference in total energy between the interface and its isolated slabs:

$$\mathcal{W}_{ad} = \sigma_{1v} + \sigma_{2v} - \sigma_{12} = (E_1^{tot} + E_2^{tot} - E_{12}^{tot}) / A. \quad (1)$$

Here  $\sigma_{iv}$  is the surface energy of slab  $i$ ,  $\sigma_{12}$  is the interface energy,  $E_i^{tot}$  is the total energy of slab  $i$ , and  $E_{12}^{tot}$  is the total energy of the interface system.  $A$  represents the *total* interface area.

One industrially relevant metal/ceramic interface is that between Aluminum and its native oxide,  $\text{Al}_2\text{O}_3$ . Aluminum is one of the world's most widely used metals, in large part due to its superior strength-to-weight ratio, but also because of the favorable protective properties afforded by its oxide layer. This layer is predominantly amorphous,[12] with a thickness ranging from 3-6 nm, and consists of  $\text{AlO}_4$  tetrahedra with a small number of  $\text{AlO}_6$  octahedra.[3] Because of the difficulties associated with modeling an amorphous oxide/metal interface, for this study we have made a simplifying approximation by substituting the amorphous oxide with its thermodynamically stable phase,  $\alpha\text{-Al}_2\text{O}_3$ . We believe this (admittedly) model system still embodies much of the essential physics of the true  $\text{Al}/\text{Al}_2\text{O}_3$  interface. Despite its importance, there have been surprisingly few theoretical studies of the electronic structure of this system, with only one *ab initio* calculation[13] appearing during the preparation of this manuscript.

As  $\mathcal{W}_{\text{ad}}$  depends upon the bond character at a given interface, the goal of this work is to systematically analyze the electronic structure of the  $\text{Al}/\alpha\text{-Al}_2\text{O}_3$  system. Unfortunately, there is currently no general model that can accurately describe bonding between metals and ceramics. An understanding of these issues would serve as an important first step in understanding the mechanical properties of metal-ceramic interfaces and to formulating a general theory of adhesion.

## METHODOLOGY

For this study we have utilized the Vienna *ab initio* Simulation Package (VASP)[2]. Two separate approximations to the exchange-correlation energy were employed: the traditional Local Density Approximation (LDA)[8] and the Generalized Gradient Approximation (GGA)[7] (PW91). All relevant quantities were carefully checked for convergence with respect to plane-wave cutoff energy and  $\mathbf{k}$ -point sampling. To test our methods, we calculated several bulk and surface properties of Al and  $\alpha\text{-Al}_2\text{O}_3$ . Very good agreement with experiment and other first-principles calculations was obtained.

As our model of the  $\text{Al}(111)/\alpha\text{-Al}_2\text{O}_3$  interface we use a fully relaxed structure (all atomic forces minimized to a tolerance of  $0.05 \text{ eV}/\text{\AA}$  or less) generated in an earlier investigation[11]. This model utilizes a 15 layer slab of  $\alpha\text{-Al}_2\text{O}_3$  (0001) arranged in a multilayer geometry between two 5 layer slabs of  $\text{Al}(111)$  with the following orientation relationship:  $(0001)_{\text{Al}_2\text{O}_3} \parallel (111)_{\text{Al}}$  and  $[10\bar{1}0]_{\text{Al}_2\text{O}_3} \parallel [\bar{1}10]_{\text{Al}}$ [5]. There is a  $10\text{\AA}$  vacuum region separating the free surfaces at the back of the Al slabs. Care has been taken to insure that the two interfaces are identical, and the lateral dimensions of the Al slab were compressed by 3.1% to match the surface unit cell of the oxide. The oxide was chosen to be terminated a monolayer of Al, as this is the preferred termination of the clean surface. A search over rigid translations of the relative positions of the slabs yielded an optimal geometry in which the metal slab's interfacial atoms were situated above the cation sites in the oxide. Both the starting (unrelaxed) and final (relaxed) interfacial structures are shown in Fig. 1. A more detailed description of this model, including a determination of adhesion energies for other oxide terminations, can be found in Ref. [11].

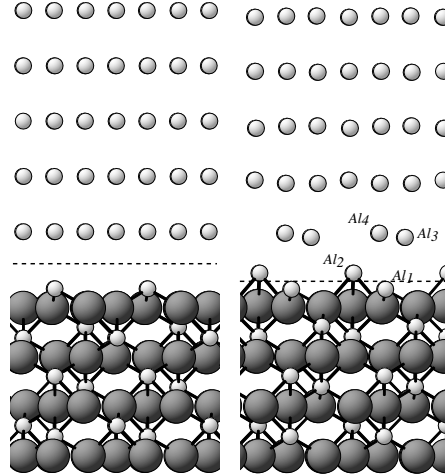


Figure 1: Left: geometry of the initial unrelaxed interface; and, right: the relaxed structure. Small spheres represent Al atoms, large spheres represent O atoms. The direction of view is along  $[1\bar{2}10]$ , and the location of the interface is indicated with a dashed line. The interfacial Al atoms are labeled according to their height above the interfacial O-layer ( $O_1$ ). The lower portion of the structure has been omitted.

## RESULTS: INTERFACIAL BONDING

### Electron Localization

The so-called “electron localization function” (ELF)[10] allows one to identify regions of space having a high concentration of paired and unpaired electrons which can subsequently be interpreted as bonds, lone pairs, and dangling bonds. Depending on the topology and magnitude of the ELF it is also possible to distinguish between metallic, covalent, and ionic bonding types.

Figure 2 shows contour plots of the ELF data through two slices of the relaxed interface along the  $(10\bar{1}0)$  and  $(11\bar{2}0)$  planes. The magnitude of the ELF in the figure is given by a grey-scale color coding in which low values are represented by black, intermediate values by increasingly lighter shades of grey, and high values by white. The  $(10\bar{1}0)$  slice clearly illustrates the nature of the bonding between the  $O_1$ -layer and the subsumed  $Al_2$  atom. In comparing the behavior of the ELF near the  $Al_2-O_1$  bond with that of the Al–O bonds deeper into the oxide, we see that they are practically *identical*: most of the charge remains localized on the  $O_1$  atoms, with distortions of the ELF attractor directed towards the  $Al_2$  atom. This shows that the  $Al_2$  atom has an electronic structure approaching that of the cations in bulk alumina, and suggests that a main contribution to Al–O interfacial bonding is of a mixed ionic-covalent type similar to what is seen in bulk alumina.

Figure 2 also gives evidence for Al–Al covalent bonding across the metal/ceramic interface. This can be seen in the  $(11\bar{2}0)$  plane as the prominent white region between the  $Al_4$  atom and the  $Al_1$ -layer. Additionally, there is another backbonding covalent-type ELF attractor between the  $Al_2$  atom and a neighboring atom in the metal slab ( $Al_4$ ), which is just barely visible in the  $(10\bar{1}0)$  slice.

Finally, our ELF analysis indicates that atomic relaxation within the Al slab results in the formation of a charge depletion region in the vicinity of the original (unrelaxed) position of the  $Al_2$  atom. (Note the region of low ELF above the  $Al_2$  atom in Fig. 2.) The weakened metallic bonding

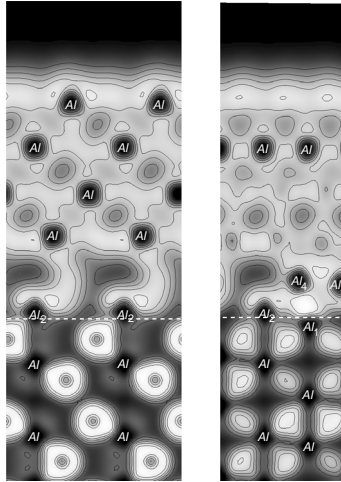


Figure 2: Two slices through the ELF for the relaxed interface along the  $(10\bar{1}0)$  (left) and  $(11\bar{2}0)$  (right) planes, showing four of the HCP O-layers in the oxide and all five atomic layers from one of the Al slabs. The position of the interface is indicated by the dashed horizontal line, and the Al atoms which intersect the contour plane are labelled.

within this region suggests a possible cleavage point for the interface. To test this hypothesis, we calculated  $\mathcal{W}_{\text{ad}}$  for cleavage between the subsumed metal atom ( $Al_2$ ) and the remainder of the metal slab. This is equivalent to a scenario in which the metal atom most strongly bound to the oxide is transferred to the oxide upon separation of the interface, *i.e.*, adhesive metal transfer. Our calculations give 2.06 (LDA)/1.63 (GGA)  $\text{J}/\text{m}^2$  for cleavage within the metal, *vs.* 1.36 (LDA)/1.06 (GGA)  $\text{J}/\text{m}^2$  at the interface, indicating that adhesive metal transfer for this interface is unlikely.

### Mulliken Population Analysis

Next, a Mulliken population analysis[6] was performed to assess the effects of ionicity and charge transfer (see Table 1). Since the absolute value of the charge populations depends sensitively upon the choice of basis set, only differences between related structures using the same basis are meaningful in establishing trends. Our Mulliken analysis was performed using the local orbital SIESTA electronic structure code,[9] with a “single zeta plus polarization” (*spd* orbitals) basis set.

The first result made clear by our population analysis is that there is a net charge transfer from the metal slabs to the oxide. With this choice of basis, we find about 0.6 electrons ( $e$ ) transferred from both Al slabs, or about  $0.3e$  per interface. By summing the charges layer-by-layer, we further find that most, if not all, of the charge lost by the metal comes only from the interfacial layer, as the remaining layers are each approximately neutral. Looking within this layer we find that it is the  $Al_2$  atom that is mainly responsible for the charge transfer, with a charge of  $+0.3e$  (see Table 1). It is interesting to note that in bulk alumina the corresponding Mulliken charge on the Al cations is  $+0.73e$ , which is slightly more than twice the value found for the  $Al_2$  atom. This seems reasonable since this atom has only half the number of nearest-neighbor oxygens (3) it would have in bulk alumina (6).

Excluding the  $Al_1$ -layer, the Mulliken population values for the remainder of the oxide atoms

	FCC	$\alpha$ -Al <sub>2</sub> O <sub>3</sub>	Al
<b>Mulliken Charge</b>			
Al <sub>1</sub>	+0.4	+0.73	
Al <sub>2</sub>	+0.3		
Al <sub>3</sub>	+0.1		
Al <sub>4</sub>	-0.1		
O <sub>1</sub>	-0.47	-0.49	
<b>Bond Order</b>			
Al <sub>1</sub> -O <sub>1</sub> ( <i>short</i> )	0.7	0.67	
Al <sub>2</sub> -O <sub>1</sub> ( <i>long</i> )	0.42	0.5	
Al <sub>1</sub> -Al <sub>2</sub>	0.15		
Al <sub>1</sub> -Al <sub>3</sub>	0.24		0.28
Al <sub>1</sub> -Al <sub>4</sub>	0.56		
Al <sub>2</sub> -Al <sub>3</sub>	0.03		
Al <sub>2</sub> -Al <sub>4</sub>	0.41		

Table 1: Bond orders and Mulliken charges for the relaxed interface compared with the bulk oxide and metal. The Al atoms are labeled as in Figs. 1, and O<sub>1</sub> refers to the interfacial O-layer.

are virtually *identical* to what is found in the bulk. This is to be expected because in the FCC stacking sequence, the interfacial O atoms are still able to maintain their 4-fold coordination by oxidizing the subsumed Al<sub>2</sub> atom. The formal charge on each O atom is approximately  $-0.47e$ , with each Al cation at  $+0.7e$ .

### Bond Order Analysis

A Mayer bond order analysis[4] can give insight regarding the relative strength of ionic and covalent/metallic bonding between a given pair of atoms. For an “appropriate” choice of basis set, a vanishing bond order between an atom pair would indicate either no bonding or a perfectly ionic bond, a value of unity would correspond to a single covalent bond, a double bond would have a value of 2, *etc.* Fractional values would then be interpreted as a mixture of ionic and covalent bonding, or metallic bonding. However, as the bond order is basis set dependent, these results should only be interpreted with respect to some other reference system.

The interfacial bonds in the relaxed FCC structure can be divided into two groups. The first set involves the three Al<sub>2</sub>-O<sub>1</sub> bonds. In our earlier ELF and Mulliken analysis, we concluded that these bonds were qualitatively similar to the long Al-O bonds found in the bulk oxide. By comparing the bond orders at the interface with those found in the bulk we can determine *how* similar they are. Our calculations give: 0.38, 0.46, and 0.43, respectively for the three bonds, for an average bond order of 0.42 (see Table 1). This is only slightly smaller than the corresponding bulk value of 0.5, thereby confirming our earlier conclusions. The deviation can be explained by differences in the bond lengths, as these bonds are all slightly longer than those found in the bulk.

The second type of interfacial bond links the oxide’s Al<sub>1</sub>-layer to an interfacial metal atom (Al<sub>4</sub>) with a relatively large bond order of 0.56. This is about twice the value of other Al-Al bonds in

the metal, and is easily seen in the  $(11\bar{2}0)$  slice of Fig. 2 as the large white region at the interface. This is a somewhat surprising result, as we did not expect to find significant bonding between the oxide's cations and the metal. It would be interesting to determine what fraction of  $\mathcal{W}_{\text{ad}}$  could be attributed to this bond, and to compare the adhesion properties of our Al/ $\alpha$ -Al<sub>2</sub>O<sub>3</sub> system to those involving other corundum-like oxides.

## CONCLUSIONS

We have conducted an *ab initio* study of the interfacial bonding at the Al(111)/ $\alpha$ -Al<sub>2</sub>O<sub>3</sub>(0001) Al-terminated metal/ceramic interface. There appear to be *two* primary bonding interactions present at the optimal interface. First, the Al–O bonds formed between the Al<sub>2</sub> atom and the alumina's O<sub>1</sub> atoms are very similar to the Al–O bonds found in the bulk oxide, and are therefore mainly ionic with a smaller degree of covalency. Secondly, there is a covalent interaction between the oxide's Al<sub>1</sub> (surface cation) layer and the Al<sub>4</sub> atom from the interfacial metal layer. Additionally, the atomic displacements within the metal's interfacial layer create small charge depletion regions that disrupt the metallic bonding. To compensate, Al–Al covalent backbonds are formed, which make cleavage within the metal unfavorable with respect to cleavage at the interface. Finally, although there is charge transfer from the metal to the oxide, within the oxide there are only small deviations from bulk-like bonding behavior.

## ACKNOWLEDGEMENTS

Computational resources were provided by the National Computational Science Alliance (NCSA) at the University of Illinois at Urbana-Champaign under grant MCA96N001N. The authors wish to thank J. Hafner for use of the VASP code, P. Ordejón for use of the SIESTA package, D. Sengupta for valuable assistance in implementing the bond order calculation, and R. Ramprasad and G. Kresse for many useful discussions. Financial support was provided by the National Science Foundation Division of Materials Research under grant DMR9619353. Additionally, D.J.S. gratefully acknowledges the General Motors Corporation for financial support during a summer internship.

## References

- [1] M. W. Finnis. *J. Phys: Cond. Mat.*, 8:5811–5836, 1996.
- [2] G. Kresse and J. Furthmüller. *Phys. Rev. B*, 54(16):11169–11186, October 1996.
- [3] P. Lamparter and R. Knierp. *Physica B*, 234:234, 1997.
- [4] I. Mayer. *Chem. Phys. Lett.*, 97(3):270–274, 1983.
- [5] D. L. Medlin, K. F. McCarty, R. Q. Hwang, S. E. Guthrie, and M. I. Baskes. *Thin Solid Films*, 299:110–114, 1997.
- [6] R. S. Mulliken. *J. Chem. Phys.*, 23:1833, 2343, 1955.
- [7] J. P. Perdew, J. A. Chevary, S. H. Vosko, et al. *Phys. Rev. B*, 46:6671, 1992.
- [8] J. P. Perdew and A. Zunger. *Phys. Rev. B*, 23(10):5048–5079, 1981.
- [9] D. Sánchez-Portal, P. Ordejón, E. Artacho, and J. M. Soler. *Int. J. Quantum Chem.*, 65:453, 1997.
- [10] Andreas Savin, Reinhard Nesper, Steffen Wengert, and Thomas F. Fässler. *Angew. Chem. Int. Ed. Engl.*, 36:1808–1832, 1997.
- [11] D. J. Siegel, Louis Jr., Hector, and J. B. Adams. submitted to *Phys. Rev. B*, 2001. preprint available at <http://ceaspub.eas.asu.edu/cms/papers/al-alumina.pdf>.
- [12] K. Wefers, G. A. Nitowski, and L. F. Weiserman. U.S. Patent 5,126,210, 1992.
- [13] W. Zhang and J. R. Smith. *Phys. Rev. Lett.*, 85:3225, 2000.